GEOPHYSICAL RESEARCH LETTERS, VOL. 34, L08807, doi:10.1029/2006GL028246, 2007

Estimating cirrus cloud properties from MIPAS data

J. Mendrok,[1,2] F. Schreier,[1] and M. Höpfner[3]

Received 21 September 2006; revised 7 February 2007; accepted 22 March 2007; published 20 April 2007.

[1] High resolution mid-infrared limb emission spectra observed by the spaceborne Michelson Interferometer for Passive Atmospheric Sounding (MIPAS) showing evidence of cloud interference are analyzed. Using the new line-by-line multiple scattering [Approximate] Spherical Atmospheric Radiative Transfer code (SARTre), a sensitivity study with respect to cirrus cloud parameters, e.g., optical thickness and particle size distribution, is performed. Cirrus properties are estimated by fitting spectra in three distinct microwindows between 8 and 12 μm. For a cirrus with extremely low ice water path (IWP = 0.1 g/m^2) and small effective particle size (D_e = 10 μm) simulated spectra are in close agreement with observations in broadband signal and fine structures. We show that a multi-microwindow technique enhances reliability of MIPAS cirrus retrievals compared to single microwindow methods. **Citation:** Mendrok, J., F. Schreier, and M. Höpfner (2007), Estimating cirrus cloud properties from MIPAS data, *Geophys. Res. Lett.*, *34*, L08807, doi:10.1029/2006GL028246.

1. Introduction

[2] Several aspects of atmospheric science evoke interest in clouds in general and ice clouds in particular. Permanently covering one third of the globe [*Wylie et al.*, 1994], cirrus clouds play an important role in the global energy balance and have to be adequately represented in climate models. Thus, global and comprehensive data of cloud occurrence and properties are highly desirable. On the other hand, clouds ''contaminate'' molecular emission and absorption spectra, thus complicate trace gas retrievals.

[3] Limb observations are well established in passive atmospheric remote sensing. Spaceborne emission sounding instruments, e.g., MIPAS on ENVISAT and MLS on EOS-Aura are successfully used for retrieval of temperature and trace gas profiles. Radiative transfer (RT) models traditionally used for Level 2 processing of limb emission sounders solve the Schwarzschild equation, i.e., consider extinction by molecular absorption only and thermal emission as the sole source. Only recently the potential of limb sounding of high altitude clouds had been examined [*Spang et al.*, 2002]. *Höpfner et al.* [2002] demonstrated that certain features in high resolution infrared (IR) limb spectra of clouds can only be explained by scattering of radiation into the line of sight (LoS). Cirrus properties have been derived from MIPAS data by *Ewen et al.* [2005], using a single microwindow at 940 – 950 cm^{-1} and ignoring the occurrence of a subjacent cloud cover.

[4] Only few line-by-line RT codes are capable of modeling multiple scattering in spherical atmospheres, e.g., ARTS [*Emde et al.*, 2004] and McClouds FM [*Ewen et al.*, 2005]. While these are pure IR and microwave RT models, the SARTre model [*Mendrok*, 2006] provides a consistent tool for terrestrial and solar radiative transfer.

[5] SARTre is used to study effects of thin cirrus clouds on IR limb spectra. An estimation of cirrus properties from MIPAS measurements and SARTre calculations is demonstrated and discussed. The article is organized as follows: section 2 briefly introduces the radiative transfer model, section 3 describes the analyzed data, and sections 4 and 5 present the sensitivity study and derivation of cirrus parameters. Conclusions are drawn in section 6.

2. The SARTre Model

[6] SARTre is designed for monochromatic high resolution RT modeling in the infrared spectral range and beyond for arbitrary viewing geometries in spherical atmospheres, taking emission and scattering into account as sources.

[7] Unlike plane-parallel scattering models, that derive the atmospheric radiation field by solving a coupled system of integro-differential equations, most spherical models, and SARTre in particular, apply the source function integration technique. Using the integral radiative transfer equation

$$I(\nu) = I_b(\nu)\, e^{-\tau(\nu)} + \int_0^{\tau(\nu)} J(\tau', \nu)\, e^{-\tau'(\nu)}\, d\tau' \qquad (1)$$

radiation sources are ''collected'' along the observer LoS and transmitted to the instrument following Beer's law. Here $I(\nu)$ is the monochromatic intensity at wavenumber ν, I_b denotes background radiation, e.g., emission of the cold space, and τ is the optical depth, measured from the observer along the LoS. The source term

$$J = J_B + J_{SS} + J_{MS} \qquad (2)$$

comprises thermal emission (B), single scattered solar radiation (SS), and multiple scattering (MS). The diffuse incident radiation field required for the calculation of the multiple scattering source J_{MS} is derived assuming a locally plane-parallel atmosphere and obtained using the pseudo-spherical version PSDISORT [*Dahlback and Stamnes*, 1991] of the radiative transfer solver DISORT [*Stamnes et al.*, 1988].

[8] Aerosol and cloud optical properties are taken from external sources. Molecular absorption is computed by line-

[1]Remote Sensing Technology Institute, German Aerospace Center, Oberpfaffenhofen, Germany.

[2]Now at Applied Electromagnetic Research Center, National Institute of Information and Communications Technology, Tokyo, Japan.

[3]Institute for Meteorology and Climate Research, Forschungszentrum Karlsruhe, Karlsruhe, Germany.

0094-8276/07/2006GL028246$05.00

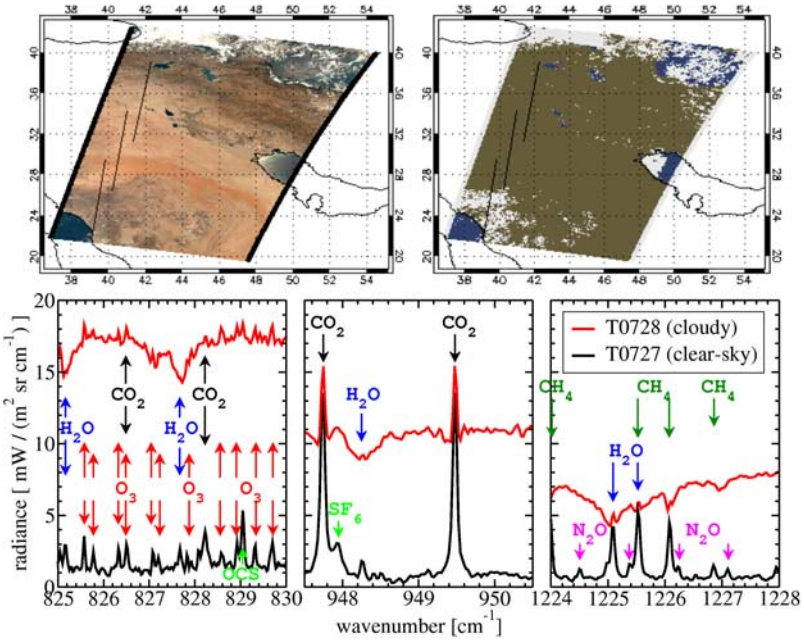

Figure 1. ENVISAT cloud observations of orbit 7203 over the Arabian Peninsula. (top) MERIS (left) RGB-composite and (right) cloud mask, courtesy of Institute for Space Sciences, Freie Universität Berlin. Time offset to MIPAS < 15 min. Overlaid middle black line indicates the LoS of the evaluated MIPAS sweeps. (bottom) MIPAS spectra ($z_{tan} \approx 15$ km) of clear-sky and cloudy conditions. Note the absorption features of H_2O and CH_4 in the cloudy spectra.

by-line routines adapted from the MIRART code [*Schreier and Böttger*, 2003] using spectral line catalogs, e.g., HITRAN [*Rothman et al.*, 2005], and optionally including continuum corrections, e.g., from *Clough et al.* [1989].

[9] SARTre has been verified by model intercomparisons to MIRART, KOPRA [*Höpfner*, 2004] and ARTS in the mid-IR and to McSCIA [*Spada et al.*, 2006] in the ultraviolet spectral region.

3. Data

[10] MIPAS [*Fischer and Oelhaf*, 1996] is a high resolution Fourier transform spectrometer onboard the European ENVISAT mission. Designed for monitoring trace gas species MIPAS measures mid-IR limb emission spectra in five channels covering 685 – 2410 cm^{-1}. A limb sequence consists of 17 so-called sweeps with nominal tangent altitudes z_{tan} of 67 km down to 6 km.

[11] For this study upper tropospheric MIPAS spectra were chosen showing distinct spectral features of thin high altitude clouds, i.e., (1) a significantly increased broadband continuum signal in the region of atmospheric windows, and (2) broad absorption line structures in place of narrow emission lines in clear-sky spectra, e.g., for H_2O lines. Candidate limb sequences selected on the basis of MIPAS cloud indices [*Spang et al.*, 2004] that represent criterion (1) were visually inspected with respect to criterion (2). To assure absence of a cloud cover below the cirrus, the MERIS cloud mask [*Santer et al.*, 1997] was evaluated in the larger vicinity of tropospheric segments of the MIPAS LoS.

[12] From a limb sequence of orbit 7203 (17 July 2003) taken over the Arabian Peninsula (30°N 41°E) sweeps 13 ($z_{tan} \approx 15$ km) and 14 ($z_{tan} \approx 12$ km) are chosen (Figure 1) to examine cirrus effects and demonstrate the derivation of cirrus properties.

4. Sensitivity Study

[13] In order to estimate properties of the observed cirrus, the sensitivity of IR limb spectra to effects of diverse cirrus parameters is examined.

[14] Similar to the analysis of MIPAS data concerning polar stratospheric clouds by *Höpfner et al.* [2002], three microwindows from channels A and B are chosen (Figure 1). Located in the atmospheric window region at 825 – 830 cm^{-1} (mw1), 947.5 – 950.5 cm^{-1} (mw2) and 1224 – 1228 cm^{-1} (mw3), they cover the ice absorption band centered around 12 μm. Note that mw2 is similar to the spectral interval used by *Ewen et al.* [2005].

[15] MIPAS cloud indices clearly indicate sweep 13 ($z_{tan} \approx$ 15 km) as the highest spectrum contaminated by clouds. Taking into account the instrument's field of view (FoV), the cloud top height is roughly estimated as $14.0 \leq z_{top} \leq 16.5$ km.

[16] Although SARTre is essentially a one dimensional (1D) spherical shell atmosphere model, it offers the option to place the cloud on one side of the LoS divided by the tangent point only. This option is of crucial importance for modeling limb observations of thin clouds with tangent altitudes below the cloud bottom: In a 1D atmosphere a limb LoS crosses the cloud layer twice and both cloud parts can contribute significantly to simulated total radiance. In "real" atmospheres it is unlikely that the same cloud is observed over the distance of tens to hundreds of kilometers between the crossing points.

[17] The cloud is assumed to consist of columnar particles and characterized by a single size distribution representative of the entire cloud body. Single scattering

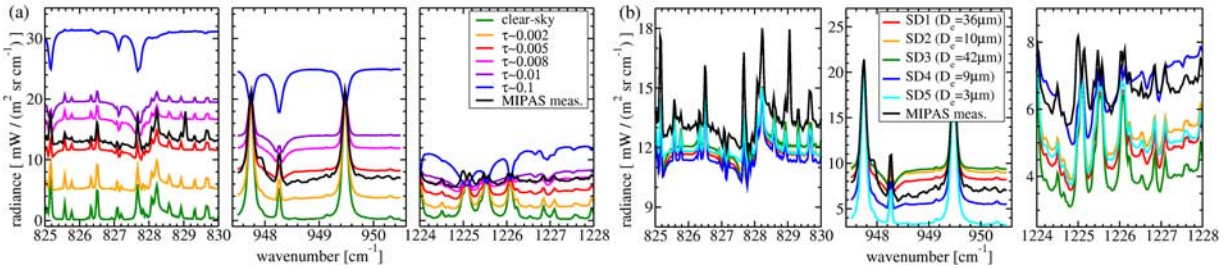

Figure 2. Sensitivity of limb mid-IR spectra ($z_{tan} \approx 12$ km) (a) to cloud optical thickness (size distribution SD1, see auxiliary material) and (b) to particle size distribution ($\bar{\tau}_c = 0.005$). Note the missing absorption features in mw1/mw2 of Figure 2b for SD5 (characterized by very small $D_e = 3$ μm) that correspond to a low single scattering albedo in these microwindows (for details see auxiliary material).

properties of individual ice crystals are taken from a database by *Yang et al.* [2005]. Five particle size distributions (SD1 – SD5) from *Liou* [1992] and *Shettle* [1989] with effective size D_e of 3 – 42 μm are applied to derive bulk optical properties (see auxiliary material[1] for details).

[18] This work focuses on cirrus effects, hence other atmospheric conditions such as temperature, pressure, and trace gas profiles are assumed to be well known. Only major contributing molecules are taken into account, i.e., H_2O, O_3, and CO_2 in mw1 and mw2, and additionally CH_4 and N_2O in mw3. Profiles retrieved from the examined MIPAS limb sequence are used [*von Clarmann et al.*, 2003], except for CO_2, where the US standard profile is scaled to 370 ppmv. Since no retrieval in case of cloud contaminated spectra is performed yet, a priori data from climatology is used for the lower atmosphere. Surface emissivity is taken from the ASTER spectral library (http://speclib.jpl.nasa.gov).

[19] The limb geometry is characterized by observer position taken from MIPAS Level 1B data and tangent altitude, using Level 1B tangent altitudes corrected by extrapolated differences to retrieved tangent altitudes. The instrument's FoV is described by a trapezoid-like function with a base of about 4 km at the tangent point [*Nett*, 2003]. As the MIPAS measurements, simulated monochromatic spectra are convolved with an instrumental line shape assuming *Norton and Beer* [1976] strong apodization.

[20] Effects of cloud properties, e.g., ice water path IWP and vertical cloud optical thickness τ_c, effective particle size D_e or size distribution, and others are studied. Among them IWP and τ_c cause the largest variability in the spectra. While being closely linked, in the mid-IR their relation highly depends on size distribution and crystal habit, i.e., a certain IWP may translate to a wide range of τ_c.

[21] Calculations for thin clouds with $0.002 \leq \bar{\tau}_c \leq 0.1$ are performed, where $\bar{\tau}_c = \sum_i \tau_c^{mwi}/3$ represents the mean optical depth of the cloud in the three microwindows, while other parameters are fixed. With increasing cloud optical thickness, a successive increase of the continuum signal is observed (Figure 2a). Water vapor absorption features show up for $\bar{\tau}_c \geq 0.005$ in form of side lobes and as inverse H_2O lines for $\bar{\tau}_c \geq 0.01$. In addition, in mw3 absorption features also occur for CH_4. Comparing simulated and measured spectra at mw1 and mw2, $\bar{\tau}_c \approx 0.005$ is estimated, whereas broadband features in mw3 suggest $\bar{\tau}_c \approx 0.008$.

[22] Results for varied size distribution with fixed mean optical thickness $\bar{\tau}_c$ are presented in Figure 2b. Note that varying the size distribution may change broadband intensity differently between the microwindows, e.g., compare SD3 and SD4 in Figure 2b. This spectral sensitivity allows estimation of particle size. In particular, fitting a proper particle size is expected to largely correct deviating estimates of $\bar{\tau}_c$ from mw1/mw2 and mw3.

[23] For thin ice clouds, several parameters like cloud top height and geometrical thickness are found to primarily result in offsetting the broadband signal over the atmospheric window, i.e., effects similar to those causes by small changes in τ_c. In contrast, the size distribution and shape of the ice particles are found to cause relative changes of the broadband intensity in the three microwindows. While the determination of cloud properties from a single microwindow as used by *Ewen et al.* [2005] is highly ambiguous since effects of particle size and shape are hardly separable from other parameters, the retrieval from microwindows placed over a wider spectral range is more reliable.

5. Cirrus Retrieval Results

[24] Cirrus properties are simultaneously derived from sweep 13 ($z_{tan} \approx 15$ km) and 14 ($z_{tan} \approx 12$ km) MIPAS measurements assuming both observe the same, homogeneous cloud. The best fit of measured and modeled spectra is obtained by minimizing the noise weighted squared residuals over the 3 microwindows for the two subsequent sweeps. It is found for a cloud with IWP = 0.1 g/m^2, $\bar{\tau}_c = 0.008$, and size distribution SD2 ($D_e = 10$ μm), that has a geometrical thickness $\Delta z = 1.0$ km with top height $z_{top} = 15.5$ km. For sweep 14 pointing below the cloud, it is located in front of the tangent point. Corresponding simulated spectra together with the MIPAS measurements are presented in Figure 3a. To illustrate the importance of scattering that accounts for 40 – 90% of the broadband radiation of the analyzed spectra, model results for clear-sky and cloudy conditions, but scattering neglected, are plotted for comparison. Residuals are shown in Figure 3b.

[25] Best fit simulations largely agree with observed spectra within the measurement accuracy for sweep 13 as well as for mw1 and mw2 of sweep 14. Beside matching the broadband intensity, the water vapor signatures observed in

[1] Auxiliary material data sets are available at ftp://ftp.agu.org/apend/gl/2006gl028246. Other auxiliary material files are in the HTML.

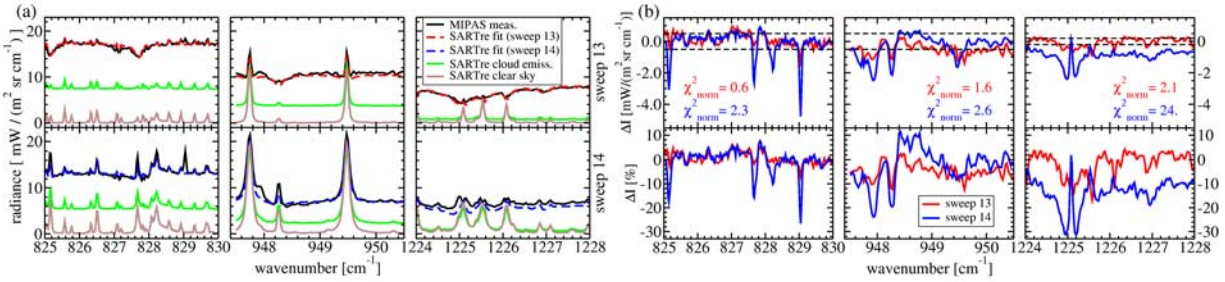

Figure 3. Fitting results. (a) Measured and modeled spectra for (top) sweep 13 and (bottom) 14. Modeled spectra for clear-sky and cloudy conditions with scattering contributions neglected are plotted for comparison. (b) Residuals (top) in intensity units (black lines indicate channel specific noise equivalent spectral radiances of MIPAS) and (bottom) relative to the measurement. Normalized noise weighted squared residuals χ_{norm}^2 are given for the 3 microwindows of both sweeps.

the MIPAS spectra are reproduced well. However, modeled intensities differ clearly from the measurement around an OCS line in mw1 and an SF_6 line in mw2, that were not included in the simulation. The underestimation of the broadband signal in mw3 of sweep 14 might be caused by spatial variations of the effective size within the cloud, while deviations around the water vapor features are likely due to uncertainties of the H_2O profile, which become more evident due to stronger H_2O interference in this microwindow. As no trace gas retrieval has been done from cloudy observations, the profiles below 18 km resemble midlatitude climatology and might differ significantly from actual conditions.

[26] A validation of SARTre retrieved cloud properties is not possible for lack of proper in-situ data. However, the properties derived for the observed cirrus cloud seem plausible. With z_{top} = 15.5 km the cloud is located right below the tropopause. Due to low ambient temperature small particles are expected to dominate, matching the finding of $D_{\mathrm{e}} \approx 10$ μm. With its extremely low IWP, the cirrus has not been detected from nearly coincident nadir observations by MERIS and MODIS.

6. Summary and Conclusions

[27] The new radiative transfer model SARTre for modeling of scattering and emission in spherical atmospheres has been used for studying effects of cirrus clouds on mid-IR limb spectra and applied for the derivation of cirrus properties from MIPAS measurements.

[28] Cloud micro- and macrophysical properties were estimated by fitting simulated spectra to MIPAS measurements simultaneously in three microwindows between 825 – 1230 cm^{-1} and two subsequent tangent altitudes. Fitted spectra matched the measurement well in both, the broadband intensity and distinct H_2O absorption features caused by scattering of radiation into the LoS. Remaining deviations between modeled and MIPAS spectra have been discussed, as well as the plausibility of the estimated cloud properties. It has been demonstrated that microwindows placed over an ice absorption band allow for the separation of effects from cloud optical thickness and particle size, which is hardly possible from a narrow spectral interval.

[29] Noise induced random errors of the derived cloud parameters are small (e.g., 0.3% for $\bar{\tau}_{\mathrm{c}}$, 0.02 km for Δz, and 0.01 km for z_{top}) due to the low instrumental noise of MIPAS as well as the large number of spectral grid points used for the retrieval. Thus, uncertainties in the atmospheric and surface parameters, and assumptions on micro- and macrophysical properties of the cirrus have to be considered as major error sources. Quantification of these will be subject to more detailed retrieval studies.

[30] Being able to model major characteristics of cloud influenced IR limb spectra, high resolution line-by-line multiple scattering radiative transfer codes like SARTre can not only be used for the derivation of cloud properties as demonstrated here, but may help to overcome the problem of trace gas retrieval in occurrence of ice clouds. However, to apply the technique for operational cloud measurements optimizations in microwindow size and positioning would be necessary as well as the implementation of a proper size distribution parameterization.

[31] **Acknowledgments.** We are grateful to Rene Preusker and his colleagues at Freie Universität Berlin for providing MERIS RGB and cloud mask data. We would like to thank two anonymous reviewers for their constructive comments and valuable suggestions. Jana Mendrok would also like to thank Jürgen Fischer at Freie Universität Berlin and Thomas Trautmann as well as Ute Böttger at German Aerospace Center for supporting this study and helpful discussions.

References

Clough, S., F. Kneizys, and R. Davies (1989), Line shape and the water vapor continuum, *Atmos. Res.*, *23*, 229–241.

Dahlback, A., and K. Stamnes (1991), A new spherical model for computing the radiation field available for photolysis and heating at twilight, *Planet. Space Sci.*, *39*(5), 671–683.

Emde, C., S. A. Buehler, C. Davis, P. Eriksson, T. R. Sreerekha, and C. Teichmann (2004), A polarized discrete ordinate scattering model for simulations of limb and nadir long-wave measurements in 1-D/3-D spherical atmospheres, *J. Geophys. Res.*, *109*, D24207, doi:10.1029/2004JD005140.

Ewen, G. B. L., R. G. Grainger, A. Lambert, and A. J. Baran (2005), Infrared radiative transfer modelling in a 3D scattering cloudy atmosphere: Application to limb sounding measurements of cirrus, *J. Quant. Spectrosc. Radiat. Transfer*, *96*(1), 45–74, doi:10.1016/j.jqsrt.2004.12.033.

Fischer, H., and H. Oelhaf (1996), Remote sensing of vertical profiles of atmospheric trace constituents with MIPAS limb-emission spectrometers, *Appl. Opt.*, *35*, 2787–2796.

Höpfner, M. (2004), Study on the impact of polar stratospheric clouds on high resolution mid-IR limb emission spectra, *J. Quant. Spectrosc. Radiat. Transfer*, *83*(1), 93–107, doi:10.1016/S0022-4073(02)00299-6.

Höpfner, M., et al. (2002), Evidence of scattering of tropospheric radiation by PSCs in mid-IR limb emission spectra: MIPAS-B observations and KOPRA simulations, *Geophys. Res. Lett.*, *29*(8), 1278, doi:10.1029/2001GL014443.

Liou, K.-N. (1992), *Radiation and Cloud Processes in the Atmosphere*, Oxford Univ. Press, New York.

Mendrok, J. (2006), The SARTre model for radiative transfer in spherical atmospheres and its application to the derivation of cirrus cloud properties, Ph.D. thesis, Freie Univ., Berlin.

Nett, H. (2003), MIPAS in-flight LOS calibration and FOV alignment verification, *ESA Rep. PO-RP-ESA-GS-1369*, Eur. Space Agency, Paris.

Norton, R., and R. Beer (1976), New apodozing functions in Fourier spectrometry, *J. Opt. Soc. Am.*, *66*, 259–264.

Rothman, L., et al. (2005), The HITRAN 2004 molecular spectroscopic database, *J. Quant. Spectrosc. Radiat. Transfer*, *96*(2), 139–204, doi:10.1016/j.jqsrt.2004.10.008.

Santer, R., V. Carrère, D. Dassailly, P. Dubuisson, and J.-C. Roger (1997), Pixel indentification, algorithm theoretical basis document (ATBD) 2.17, *ESA Doc. PO-TN-MEL-GS-0005*, Eur. Space Agency, Paris.

Schreier, F., and U. Böttger (2003), MIRART, a line-by-line code for infrared atmospheric radiation computations incl. derivatives, *Atmos. Oceanic Opt.*, *16*, 262–268.

Shettle, E. (1989), Models of aerosols, clouds and precipitation for atmospheric propagation studies, paper presented at Conference on Atmospheric Propagation in the UV, Visible, IR and MM–Wave Region and Related Systems Aspects, AGARD, Copenhagen, 9–13 Oct.

Spada, F., M. Krol, and P. Stammes (2006), McSCIA: Application of the Equivalence Theorem in a Monte Carlo radiative transfer model for spherical shell atmospheres, *Atmos. Chem. Phys.*, *6*(12), 4823–4842.

Spang, R., G. Eidmann, M. Riese, D. Offermann, P. Preusse, L. Pfister, and P.-H. Wang (2002), CRISTA observations of cirrus clouds around the tropopause, *J. Geophys. Res.*, *107*(D23), 8174, doi:10.1029/2001JD000698.

Spang, R., J. Remedios, and M. Barkley (2004), Colour indices for the detection and differentiation of cloud types in infra-red limb emission spectra, *Adv. Space Res.*, *33*(7), 1041–1047.

Stamnes, K., S.-C. Tsay, W. Wiscombe, and K. Jayaweera (1988), Numerically stable algorithm for discrete-ordinate-method radiative transfer in multiple scattering and emitting layered media, *Appl. Opt.*, *27*, 2502–2509.

von Clarmann, T., et al. (2003), Retrieval of temperature and tangent altitude pointing from limb emission spectra recorded from space by the Michelson Interferometer for Passive Atmospheric Sounding (MIPAS), *J. Geophys. Res.*, *108*(D23), 4736, doi:10.1029/2003JD003602.

Wylie, D., W. Menzel, H. Woolf, and K. Strabala (1994), Four years of global cirrus cloud statistics using HIRS, *J. Clim.*, *9*, 1972–1986.

Yang, P., H. Wei, H.-L. Huang, B. Baum, Y. Hu, G. Kattawar, M. Mishchenko, and Q. Fu (2005), Scattering and absorption property database for nonspherical ice particles in the near-through far-infrared spectral region, *Appl. Opt.*, *44*, 5512–5523.

M. Höpfner, Institut für Meteorologie und Klimaforschung, Forschungszentrum Karlsruhe, Postfach 3640, D-76021 Karlsruhe, Germany. (michael.hoepfner@imk.fzk.de)

J. Mendrok, Applied Electromagnetic Research Center, National Institute of Information and Communications Technology, 4-2-1 Nukui-kita, Koganei, Tokyo 184-8795, Japan. (mendrok@nict.go.jp)

F. Schreier, Remote Sensing Technology Institute, German Aerospace Center, Oberpfaffenhofen, D-82234 Weßling, Germany. (franz.schreier@dlr.de)